DOI: https://doi.org/10.24425/amm.2023.142442

V.S.S. VENKATESH[1*], KALAPALA PRASAD[2], ASHISH B. DEOGHARE[3]

CHARACTERIZATION OF MICROWAVE SINTERED ALUMINIUM COMPOSITE REINFORCED WITH HYDROXYAPATITE EXTRACTED FROM RIHU FISH SCALES

In this study, Hydroxyapatite (HAp) is extracted from the Rihu fish scales which are generally dumped as garbage. The aluminium composite was fabricated through the powder metallurgy technique by reinforcing HAp (0, 5, 10 and 15 wt%) as a reinforcement. The fabricated samples were sintered through microwave sintering at 530°C for 15 min under an argon gas environment. The fabricated composites were subjected to X-Ray Diffraction (XRD), Scanning Electron Microscopy (SEM) and Energy Dispersive Spectroscopy (EDS) analysis to confirm the constituting elements and to describe the reinforcement dispersion in the matrix. Uniform reinforcement dispersion was observed for the composite reinforces with 5%HAp, 10%HAp particles. The mechanical characterization results reveal that the Al-10% HAp composite exhibits a microhardness value of 123 ± 3 Hv and maximum ultimate tensile strength of 263 ± 10 MPa and 299 ± 9 MPa compression strength was obtained due to the presence of a strong bond among the aluminium and HAp particles.

Keywords: Hydroxyapatite; Aluminium matrix; microwave sintering; mechanical properties; Scanning Electron Microscopy

Abbreviations

U.T.S – Ultimate tensile strength,
C.S – Compressive Strength,
HAp – Hydroxyapatite,
MAS – Microwave-Assisted Sintering.

1. Introduction

Composites synthesized with naturally derived reinforcements play a vital role in the present era due to their exceptional properties like lower cost, improved mechanical and tribological properties [1]. Composite consists of a softer matrix and harder reinforcement material. Among the numerous matrix materials, aluminium is the best preferable matrix due to its inherent properties like high ductility, better corrosion resistance and low melting point [2]. Metal matrix composite can be fabricated through various fabrication processes such as powder metallurgy, stir casting and infiltration methods [3]. Among all the available techniques, the powder metallurgy process of composite synthesis produces composites with minimal porosities and uniform reinforcement distribution. In the case of the powder metallurgy route of composite synthesis, the compacted specimens were sintered using conventional, microwave-assisted sintering (MAS) and spark plasma sintering (SPS) techniques [4]. The existence of a higher heating period in conventional furnace heating is prone to oxidation of and generation of agglomerations at the interfaces of the particles. But in the MAS process, the internal heat generation from the particle leads to uniform heat dispersion and the initiation of strong bonds among the adjacent particles. Researchers develop the metal matrix composites by reinforcing naturally available particles such as coconut shell ash, cow dung powder, aloe vera particles and rice husk to enhance the mechanical characteristics of the composite [5-7]. Manikandan et al., [7] analyzed the stir-casted Al-Cowdung-B_4C composite and concluded that the presence of self-lubrication property of the cow dung particles decreases the hardness of the fabricated composites up to the addition of 10% cow dung particles. K.K. Alaneme et al., [8] studied the mechanical behaviour of the stir cast Aluminium composite incorporated with rice husk and alumina particles. The author's results reveal a decrement in U.T.S by 8% with the 3% HRA reinforcement compared to unreinforced aluminium. B. Praveen Kumar et al., [9] investigated the influence of bamboo

[1] GMR INSTITUTE OF TECHNOLOGY, RAJAM, INDIA
[2] UNIVERSITY COLLEGE OF ENGINEERING, JNTU KAKINADA, INDIA
[3] NATIONAL INSTITUTE OF TECHNOLOGY SILCHAR, ASSAM, INDIA

* Corresponding author: vssvenkateshnits@gmail.com

leaf ash (BLA) particles on the mechanical characteristics of the stir-casted Al-bamboo leaf ash composite and the results reveal that the utmost hardness of 104 Hv and U.T.S of 177 MPa was attained for 4% BLA reinforcement content.

The present work aimed to develop the composite by incorporating Hydroxyapatite (HAp) as reinforcement material. Fishes are consumed as food and their scales were dumped in the garbage as waste material. But these fish scales contain calcium and phosphorus elemental constituents which attribute to the enhancement of the mechanical properties of the composite material. Hence, this study aims to convert this waste material into a value-added product by synthesizing the aluminium composite via microwave-assisted sintering (MAS) with the incorporation of HAp which was extracted from the Rihu fish scales. The mechanical characteristics of the synthesized composite were studied by varying the wt% of HAp content in the aluminium matrix. The synthesized composite can be a prominent material for fabricating parts in automobile applications.

2. Materials and fabrication methods

2.1. Raw materials

In this work, aluminium powder (99% purity, APS ≤ 30 µm) procured from nanoshell company was used as a matrix material.

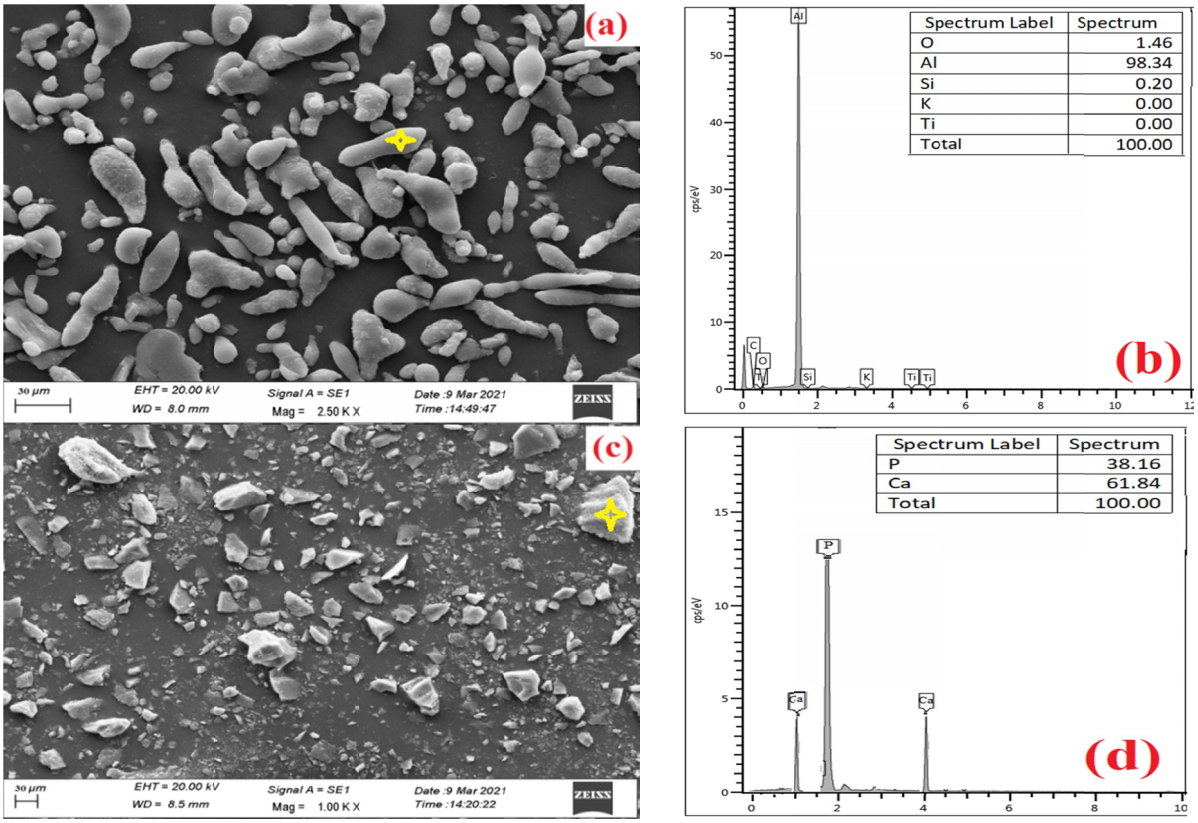

Fig. 1. Particle sizes for (a) Aluminium, (c) HAp reonforcements. (b) EDX spectrum for (b) Aluminium and (d) HAp particles

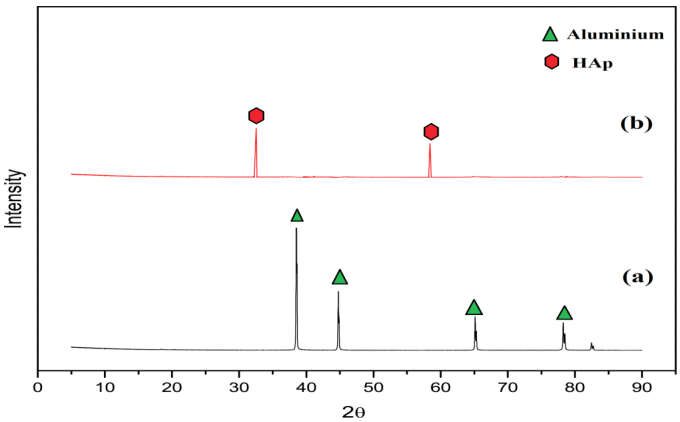

Fig. 2. XRD pattern for (a) Aluminium and (b) Synthesized Hydroxyapatite

Hydroxyapatite synthesized from Rihu fish scales (APS ≤ 30 µm) was utilized as reinforcement material. The particle sizes, EDX spectrum and XRD pattern of as received matrix and reinforcements were depicted in Fig. 1 and Fig. 2 [10] respectively.

2.2. Ball Milling

The as-received Aluminium and synthesized hydroxyapatite powders were loaded in a RESTECH100 ball mill to achieve uniform HAp dispersion and to create the strain hardening effect among the particles [11]. The HAp particles were reinforced in the aluminium with the proportion of 5%, 10% and 15% to fabricate the composite [12].

2.3. Cold compaction and composite sintering

The obtained powders from the ball mill were compacted on the manually operated Kameyo pallet press with the application of 600 MPa pressure [11]. Zinc stearate is mixed with acetone (C_3H_6O) and applied to the punch and die interfaces as a lubricating medium for the easy removal of compacted samples [13]. The ejected composite specimens were subjected to the MAS process for 500°C for 30 min with a heating rate of 10°C/min to initiate the interface bonds among the Al and HAp particles [4]. The power supply of 1.4 kW/2.45 GHz was supplied to the MAS furnace equipped with alumina insulation to avoid heat loss and to generate internal heat in the composites [14]. The synthesized composites through the MAS process for the tensile, hardness and compression tests were depicted in Fig. 3.

2.4. Extraction of Hydroxyapatite

Rihu fishes were collected from the Vishakhapatnam sea shore and removed the scales by using the fish scale scraper. The obtained scales are washed with distilled water to separate any debris that may be adhered to the scales and then sun-dried for 12 h to remove the entrapped moisture present on the fish scales. The fish scales are deproteinized for 24 h with HCl solution to remove the organic substances. After that, the scales were thoroughly cleaned in distilled water for 5 times and thereafter oven-dried at 50°C for 12 h. Calcination is performed for 4 h at 1000°C temperature to synthesize HAp [15,16]. The overall schematic diagram for the extraction of HAp is depicted in Fig. 4.

2.5. Composite Characterization

The fabricated samples were analysed for SEM investigation to reveal the reinforcement dispersion in the aluminium matrix. Prior to SEM analysis, the composites were polished on the 220, 400, 1000, and 2500 grit size abrasive papers and etched with Kellar's reagent (Mixture of 3 ml HCL + 5 ml HNO_3 + 2 ml HF + 190 ml distilled water) for the enhanced grain visualization. Tensile, compression tests were performed by using M30 micro UTM as per ASTM E8 and ASTM E9 standards with a 1 mm/min strain rate [17]. The microhardness of the composite

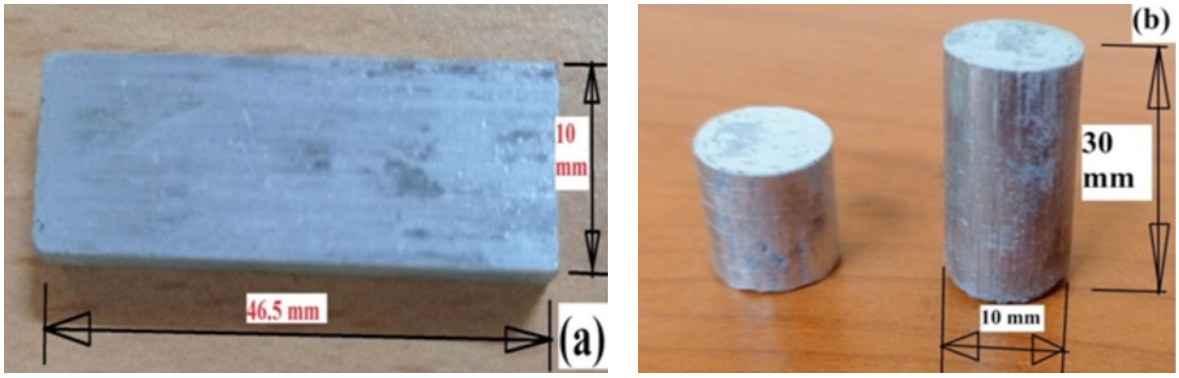

Fig. 3. Synthesized composites for the (a) Tensile, (b) Hardness and compression test

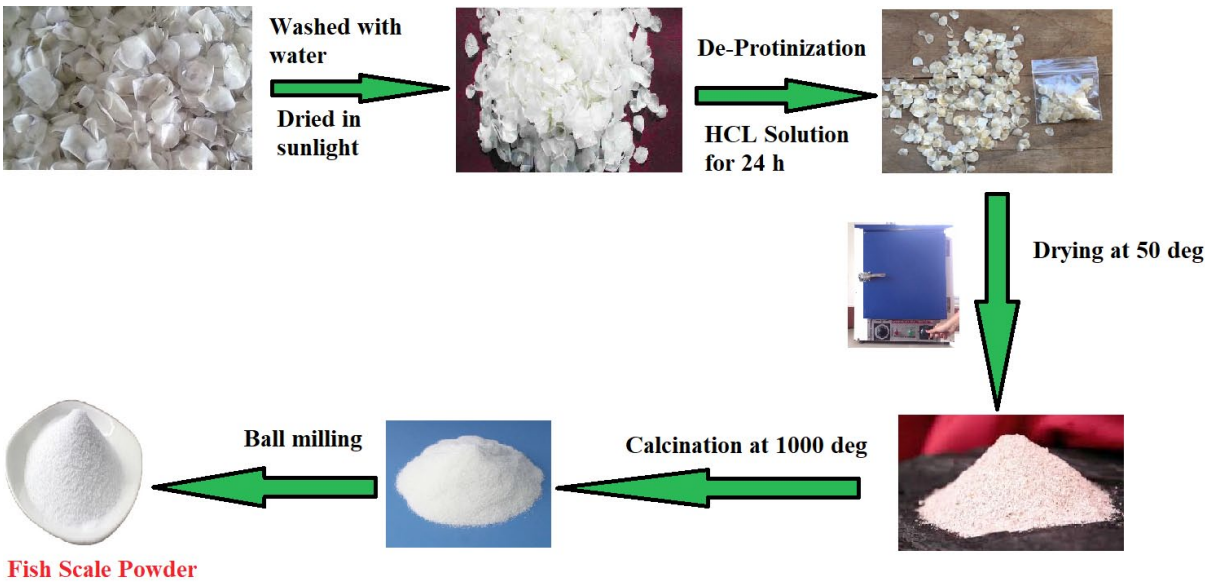

Fig. 4. Schematic diagram for extraction of Hydroxyapatite

was determined by applying a 200 g load with 15 s dwell time. Archimedes' principle was adopted to calculate the porosity of the composites [11,18]. To maximize the precision of the results, an arithmetic mean of five readings was taken.

3. Results and Discussion

3.1. XRD and Microstructural Investigation

XRD pattern for the As-received aluminium and synthesized Hydroxyapatite (HAp) is shown in Fig. 2. The obtained peaks were compared with JCPDS card numbers. The peaks obtained at the 2θ value of 39°, 44.5° confirms the presence of aluminium particles (JCPDS card number: 04-0787 [19]). The presence of HAp was identified by the peak obtained at 2θ values of 31.77°, and 27.2° (JCPDS card number: 09-0432) [16,20]. There are no signs of agglomerations present in the XRD analysis of HAp as depicted in Fig. 2. The existence of different deformation behaviour of the aluminium and the HAp reinforcements creates the triaxial stress at the interface regions [21]. The formation of $AlPO_4$ (Aluminium Phospate) intermetallic compound identified at a 2θ value of 48.92° angle for the Al-15% HAp composite sintered through MAS technique as depicted in Fig. 5 [10]. However, no agglomerations were detected in the XRD pattern of Al-10%HAp composites. The $AlPO_4$ agglomerations at the interface regions decrease the bonding intensity between the aluminium and HAp particles which impedes the load transmissibility phenomenon from the matrix to HAp reinforcements and reduces the strength of the Al-15%HAp composite [22].

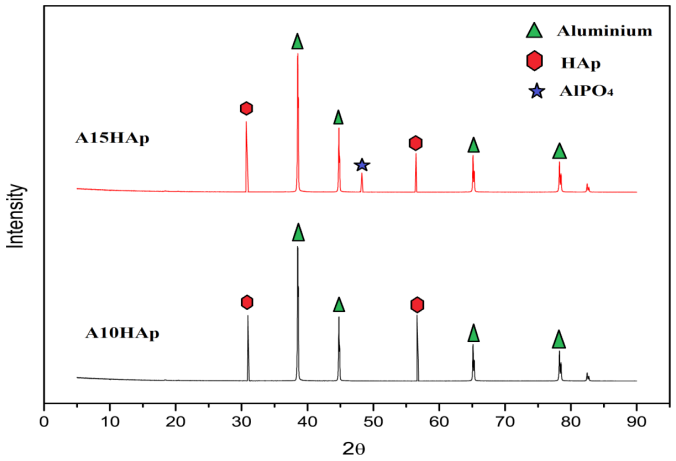

Fig. 5. XRD peaks for the fabricated Al-10% HAp and Al-15%HAp composites

The SEM images for the Microwave sintered Al-5%HAp, Al-10%HAp and Al-15%HAp were shown in Fig. 6. The HAp reinforcements were uniformly distributed and no agglomerations were identified for 5 wt% and 10 wt% HAp addition due

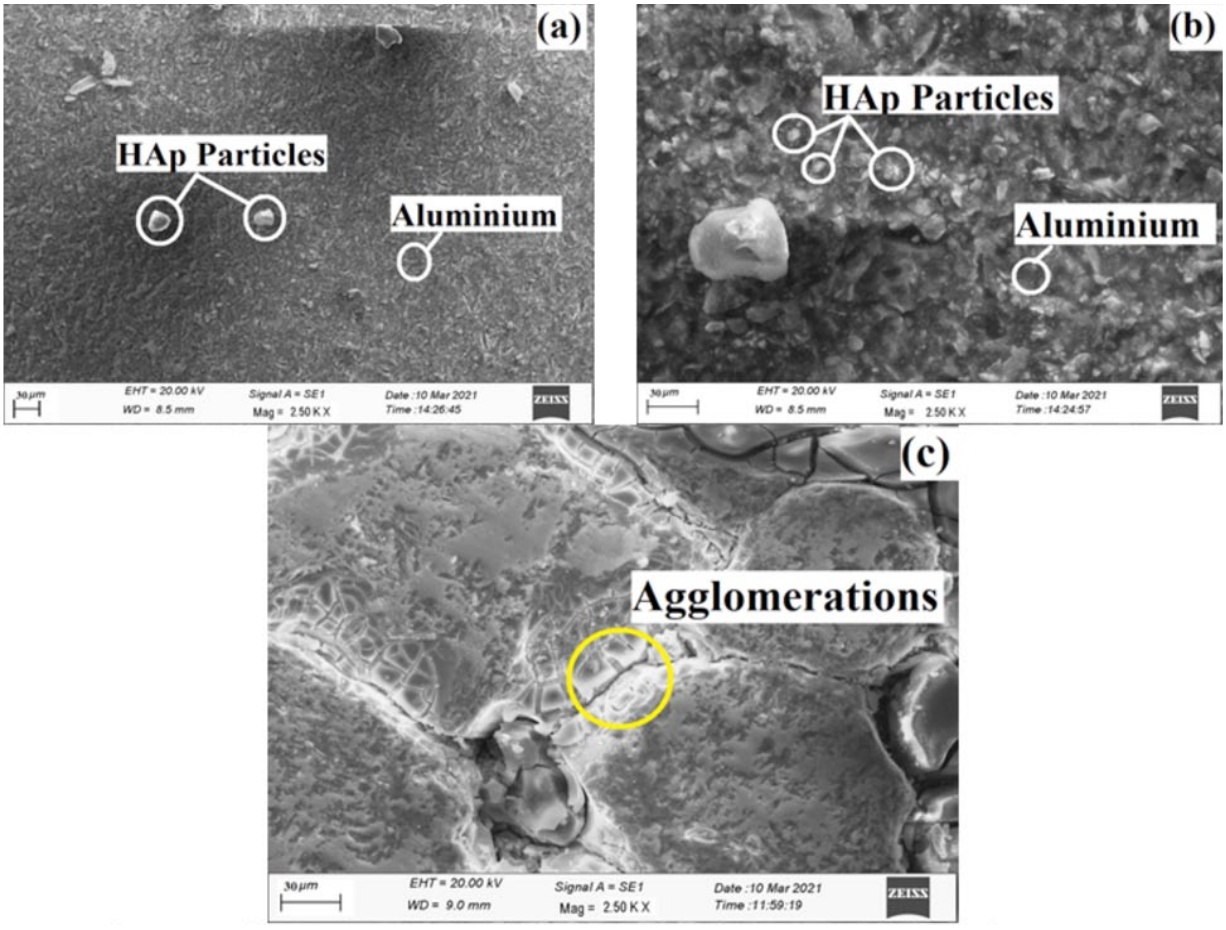

Fig. 6. SEM images for the (a) Al-5%HAp, (b) Al-10%HAp and (c) Al-15%HAp

to the faster sintering rates which enables the rapid diffusion of HAp particles among the interfaces [4,23]. However, $AlPO_4$ intermetallics were detected in the Al-15%HAp composite as a result of the strong chemical interactions among the interface particles. The existence of variation in thermal expansions of the matrix and the aluminium phosphate intermetallics leads to uneven expansions during the MAS process which deteriorates the load capability behaviour of the composite and causes the reduction in strength of the composite [24]. The HAp reinforcements hinder the dislocation movement around the grain boundaries during the composite sintering. In addition to this, the high level of clustering and formation of intermetallics at 15%HAp addition leads to the formation of pores which reduces the intensity of bonding between the adjacent particles and is prone to reduction in mechanical strength of composite at a higher % of HAp reinforcements. The SEM micrographs for the synthesized composites (Refer Fig. 6(a)-(c)) are free from voids, which confirms the aluminium matrix is free from oxidation phenomenon during the sintering process.

3.2. Porosity of the synthesized composites

The interstitial gaps that exist between the interface particles are termed porosity. The powder metallurgy technique typically results in the creation of these voids during the compaction process. The existence of porosity in the material deteriorates the interface bonding between the interface particles which negatively affects the mechanical characteristics of the composite [25]. These air gaps obstruct the heat transfer during the sintering and lead to improper sintering of the composite [26]. The porosity of a given specimen depends on the magnitude of pressure applied during the compaction stage and the densification behaviour of the as-received powders [27]. In the quasi-static condition of the compaction process, the particles have sufficient time to move and occupy the void spaces to produce the densified composite. In this present work, 600 MPa quasistatic compaction pressure was applied to synthesize the composite with minimum porosity levels. Fig. 7 depicts the % porosity for the synthesized Al-HAp composite for different wt% of HAp reinforcement. The % porosity was reduced from 3.6% to 2.9% with the incorporation of HAp wt% from 0 wt% to 10 wt%. Reinforcing HAp particles more than 10 wt% leads to increasing the porosity levels from 2.9% to 3.7%. This was attributed due to the initiation of intergranular crack propagation in the grain boundaries with the incorporation of 15wt% HAp reinforcement. The obtained porosity level at 10% HAp was 64.63% lesser than the porosity obtained for 10% kaolin clay reinforced aluminium composite sintered through conventional sintering technique [12].

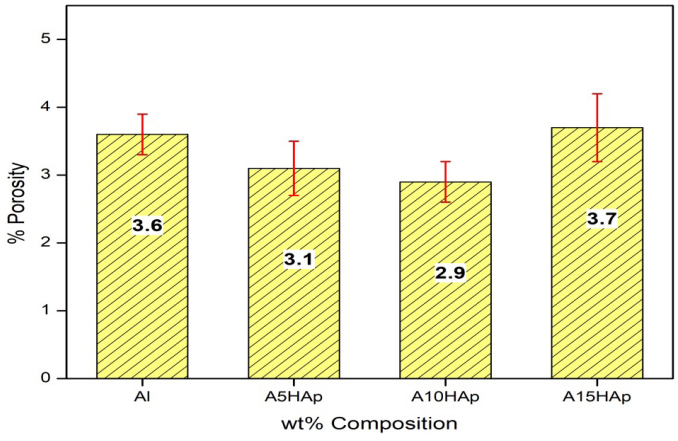

Fig. 7. Porosity for the synthesized Al-x%HAp (x = 0, 5, 10, 15)

3.3. Mechanical Properties

The variation of the hardness with wt% of HAp reinforcement was depicted in Fig. 8. The results inferred that the hardness of the synthesized composite was improved from 79 Hv to 147 Hv for the incorporation HAp reinforcement from 0% to 15% i,e an enhancement of 86.07% hardness was obtained for Al-15HAp than the pure aluminium. The enhancement in composite hardness was due to the addition of harder HAp particles (contains Ca and P) into the ductile aluminium matrix. In addition to this, the incorporated HAp reinforcements occupy the interstitial voids and offer resistance to the indenter movement which provokes the improvement in Al-HAp composite hardness with the incorporation of HAp content [28].

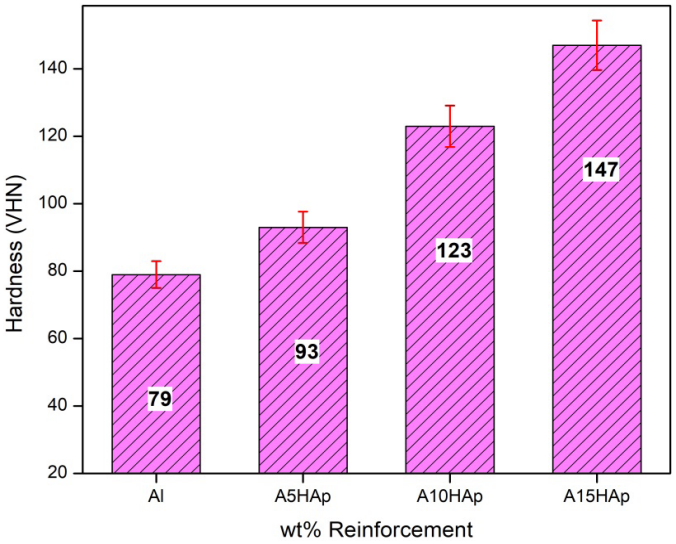

Fig. 8. Variation of hardness with wt% of HAp reinforcement

Fig. 9(a) depicts the average U.T.S and C.S of the synthesized Al-HAp composites, whereas Fig. 9(b) depicts the tensile stress-strain curve for the synthesized composites. Results concluded that there was an improvement of 46.9% in U.T.S and 64.28% in C.S of the Al-10%HAp than the unreinforced aluminium. The reinforced HAp particles generate strain fields in the vicinity of the interfaces which offers higher resistance to the movement of dislocations during the application of load which is prone to improvement in U.T.S and C.S of the synthesized composite [29]. Along with this, the uniform HAp particle dispersion in the aluminium matrix creates strong bonds with the neighbouring particles which facilitates the better load withstanding capa-

bility of the matrix and harder HAp particles. In contrast, the incorporation of 15 wt% HAp particles in the aluminium matrix decreases the U.T.S from 263 MPa to 242 MPa and compressive strength from 299 MPa to 273 MPa for 10% HAp to 15% HAp content. The decrement in the mechanical properties was attributed due to the addition of more wt% of HAp particles leading to enhance in the intensity of slip planes and the particles present along these planes can move easily at the application of lower magnitude of loads and reduces the composite strength as depicted in Fig. 9 [30]. The obtained U.T.S value at 10% HAp was higher than the U.T.S obtained with the 10wt% kaoline reinforced composite [31].

SEM investigation was performed on the tensile fractured surface to reveal the nature of the fracture that occurred in the composite. Fig. 10 illustrates the fractography images for the A5HAp, A10HAp and A15HAp composites. Dimples

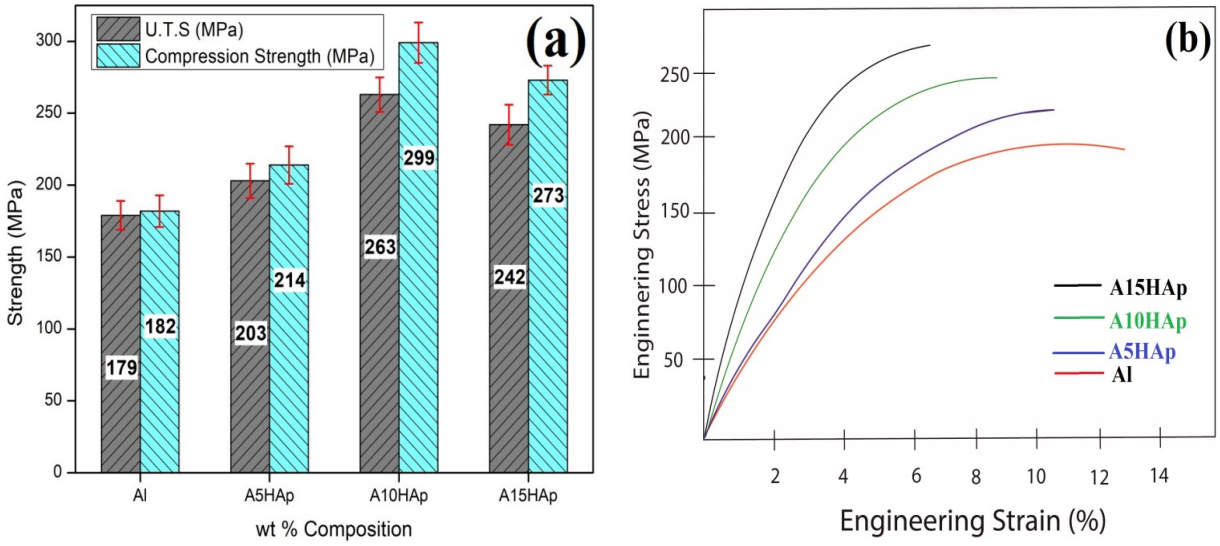

Fig. 9. (a) Variation of U.T.S and compression strength with wt% HAp reinforcement, (b) Strain-strain curve for the synthesized composite

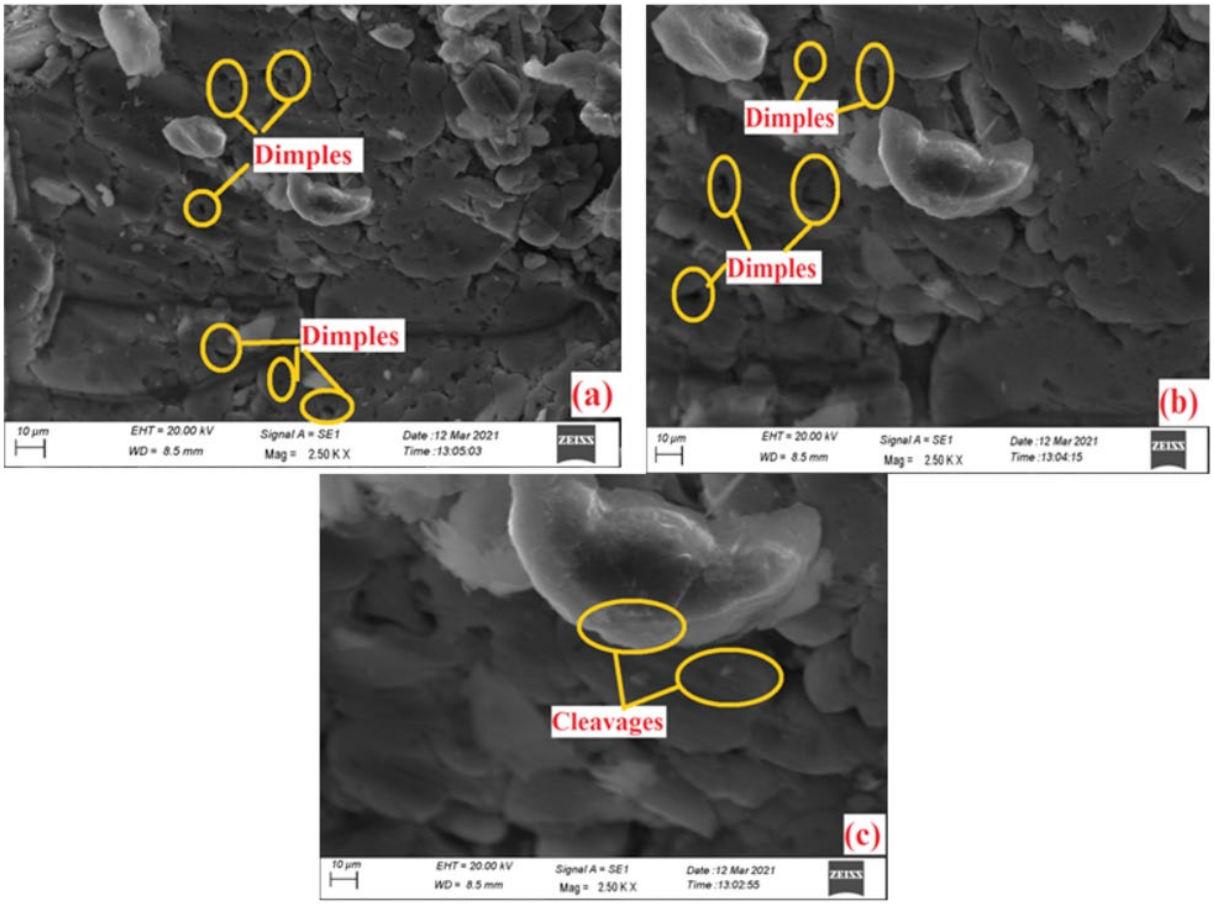

Fig. 10. SEM images for the fractured tensile composites

structure was identified on the composites for 5% and 10% HAp reinforcement which confirms the ductile fracture [32]. However, the formation of brittle agglomerations at 15% HAp leads to brittle fracture in the composite which was confirmed by the cleavage texture present on the SEM micrograph of the A15HAp composite. The existence of the harder HAp decreases the ductility of the aluminium matrix which causes the detachment and clustering of HAp particles from the matrix surface which appears as cleavage facts in the SEM micrographs. The cleavages are prone to the initiation, propagation of microcracks and brittle failure of the composite at the lesser magnitude of applied load.

4. Conclusions

The present work explored the mechanical behaviour of the microwave sintered Al-HAp composite. The novel outcomes obtained from the various mechanical characterizations were summarized below.

- The Al-HAp composites were successfully synthesized through the MAS process and the absence of porosities was identified on the SEM micrographs of the synthesized composite.
- The hardness of the synthesized composite was found to be improved from 79 Hv for pure aluminium to 147 Hv for composite with 15 wt% HAp reinforcement. This was due to the incorporation of harder Ca and P elements in the HAp reinforcement.
- SEM micrographs of the synthesized Al-5%HAp and Al-10%HAp composites reveal the uniform dispersion of HAp particles in the matrix. However, $AlPO_4$ agglomerations were identified in the composite with 15 wt% HAp reinforcements.
- The ductile fracture was observed on the fractured tensile Al-5%HAp and Al-10%HAp specimen due to the dimples formation. Despite this, cleavages were identified on the Al-15%HAp composite fractured surface.
- The internal heat generation from the particles in the MAS process enhances the mechanical characteristics of the developed Al-HAp composite and makes it suitable for automobile applications.

REFERENCES

[1] S. Das Lala, A.B. Deoghare, S. Chatterjee, Effect of reinforcements on polymer matrix bio-composites – An overview, IEEE J. Sel. Top. Quantum Electron. **25**, 1039-1058 (2018).
DOI: https://doi.org/10.1515/secm-2017-0281

[2] A. Simon, D. Lipusz, P. Baumli, P. Balint, G. Kaptay, G. Gergely, A. Sfikas, A. Lekatou, A. Karantzalis, Z. Gacsi, Microstructure and mechanical properties of Al-WC composites, Arch. Metall. Mater. **60**, 1517-1521 (2015).
DOI: https://doi.org/10.1515/amm-2015-0164.

[3] B. Leszczyńska-Madej, A. Wasik, M. Madej, Microstructure Characterization of SiC Reinforced Aluminium and Al4Cu Alloy Matrix Composites, Arch. Metall. Mater. **62**, 747-755 (2017).
DOI: https://doi.org/10.1515/amm-2017-0112

[4] P. Ashwath, M. Anthony Xavior, The effect of ball milling & reinforcement percentage on sintered samples of aluminium alloy metal matrix composites, Procedia Eng. **97**, 1027-1032 (2014).
DOI: https://doi.org/10.1016/j.proeng.2014.12.380

[5] A.K. Bledzki, A.A. Mamun, J. Volk, Barley husk and coconut shell reinforced polypropylene composites: The effect of fibre physical, chemical and surface properties, Compos. Sci. Technol. **70**, 840-846 (2010).
DOI: https://doi.org/10.1016/j.compscitech.2010.01.022

[6] V.S.S. Venkatesh, A.B. Deoghare, Effect of Particulate Type Reinforcements on Mechanical and Tribological Behavior of Aluminium Metal Matrix Composites: A Review, in: K.M. Pandey, R.D. Misra, P.K. Patowari, U.S. Dixit (Eds.), Recent Adv. Mech. Eng., Springer Singapore, Singapore, pp. 295-303, 2021.

[7] R. Manikandan, T.V. Arjunan, A.R. Akhil, Studies on micro structural characteristics, mechanical and tribological behaviours of boron carbide and cow dung ash reinforced aluminium (Al 7075) hybrid metal matrix composite, Compos. Part B Eng. **183**, 107668 (2020).
DOI: https://doi.org/10.1016/j.compositesb.2019.107668

[8] K.K. Alaneme, I.B. Akintunde, P.A. Olubambi, T.M. Adewale, Fabrication characteristics and mechanical behaviour of rice husk ash – Alumina reinforced Al-Mg-Si alloy matrix hybrid composites, J. Mater. Res. Technol. **2**, 60-67 (2013).
DOI: https://doi.org/10.1016/j.jmrt.2013.03.012

[9] B.P. Kumar, A.K. Birru, Microstructure and mechanical properties of aluminium metal matrix composites with addition of bamboo leaf ash by stir casting method, Trans. Nonferrous Met. Soc. China (English Ed. **27**, 2555-2572 (2017).
DOI: https://doi.org/10.1016/S1003-6326(17)60284-X

[10] R.H.P. Devamani, A. M., Synthesis and Characterization of Aluminium Phosphate Nanoparticles, Int. J. Appl. Sci. Eng. Res. **1**. 769-775 (2012).
DOI: https://doi.org/10.6088/ijaser.0020101078

[11] G. Manohar, K.M. Pandey, S.R. Maity, Effect of sintering mechanisms on mechanical properties of AA7075/B4C composite fabricated by powder metallurgy techniques, Ceram. Int. (2021).
DOI: https://doi.org/10.1016/j.ceramint.2021.02.073

[12] V.S.S. Venkatesh, A.B. Deoghare, Fabrication and mechanical behaviour of Al-Kaoline metal matrix composite fabricated through powder metallurgy technique, in: Mater. Today Proc., Elsevier Ltd 3291-3296 (2020).
DOI: https://doi.org/10.1016/j.matpr.2020.10.021

[13] N. Nemati, R. Khosroshahi, M. Emamy, A. Zolriasatein, Investigation of microstructure, hardness and wear properties of Al-4.5wt.% Cu-TiC nanocomposites produced by mechanical milling, Mater. Des. **32**, 3718-3729 (2011).
DOI: https://doi.org/10.1016/j.matdes.2011.03.056

[14] M. Bhattacharya, T. Basak, A review on the susceptor assisted microwave processing of materials, Energy **97**, 306-338 (2016).
DOI: https://doi.org/10.1016/j.energy.2015.11.034

[15] P. Deb, A.B. Deoghare, A. Borah, E. Barua, S. Das Lala, Scaffold Development Using Biomaterials: A Review, Mater. Today Proc. **5**, 12909-12919 (2018).
DOI: https://doi.org/10.1016/j.matpr.2018.02.276

[16] P. Deb, E. Barua, S. Das Lala, A.B. Deoghare, Synthesis of hydroxyapatite from Labeo rohita fish scale for biomedical application, Mater. Today Proc. **15**, 277-283 (2019).
DOI: https://doi.org/10.1016/j.matpr.2019.05.006

[17] V.S.S. Venkatesh, A.B. Deoghare, Modelling and Optimisation of Wear Parameters for Spark Plasma Sintered Al – SiC – Kaoline Hybrid Composite Modelling and Optimisation of Wear Parameters for Spark Plasma Sintered Al – SiC – Kaoline Hybrid Composite, Adv. Mater. Process. Technol. 1-19 (2021).
DOI: https://doi.org/10.1080/2374068X.2021.1939561

[18] M.R. Mattli, A. Shakoor, P.R. Matli, A.M.A. Mohamed, Microstructure and compressive behavior of Al–Y2O3 nanocomposites prepared by microwave-assisted mechanical alloying, Metals (Basel). **9** (2019). DOI: https://doi.org/10.3390/met9040414

[19] A. Manuscript, R. Society, A. Manuscripts, T.A. Manuscript, A. Manuscripts, R. Society, A. Manuscript, RSC Advances, (n.d.).

[20] S. Das Lala, E. Barua, P. Deb, A.B. Deoghare, Physico-chemical and biological behaviour of eggshell bio-waste derived nano-hydroxyapatite matured at different aging time, Mater. Today Commun. **27**, 102443 (2021).
DOI: https://doi.org/10.1016/j.mtcomm.2021.102443.

[21] V.S.S. Venkatesh, A.B. Deoghare, Effect of microwave sintering on the mechanical characteristics of Al / kaoline / SiC hybrid composite fabricated through powder metallurgy techniques MAS, Mater. Chem. Phys. **287**, 126276 (2022).
DOI: https://doi.org/10.1016/j.matchemphys.2022.126276

[22] Z. Zhou, B. Liu, W. Guo, A. Fu, H. Duan, W. Li, Corrosion behavior and mechanism of FeCrNi medium entropy alloy prepared by powder metallurgy, J. Alloys Compd. **867**, 159094 (2021).
DOI: https://doi.org/10.1016/j.jallcom.2021.159094

[23] F. Toptan, A. Kilicarslan, A. Karaaslan, M. Cigdem, I. Kerti, Processing and microstructural characterisation of AA 1070 and AA 6063 matrix B4Cp reinforced composites, Mater. Des. **31**, S87-S91 (2010). DOI: https://doi.org/10.1016/j.matdes.2009.11.064

[24] K. Ravi Kumar, K. Kiran, V.S. Sreebalaji, Micro structural characteristics and mechanical behaviour of aluminium matrix composites reinforced with titanium carbide, J. Alloys Compd. **723**, 795-801 (2017).
DOI: https://doi.org/10.1016/j.jallcom.2017.06.309

[25] V.S.S. Venkatesh, A.B. Deoghare, Effect of boron carbide and Kaoline reinforcements on the microstructural and mechanical characteristics of aluminium hybrid metal matrix composite fabricated through powder metallurgy technique, Adv. Mater. Process. Technol. **8**, 1007-1028 (2021).
DOI: https://doi.org/10.1080/2374068X.2021.1945314

[26] H. Alihosseini, K. Dehghani, J. Kamali, Microstructure characterization, mechanical properties, compressibility and sintering behavior of Al-B4C nanocomposite powders, Adv. Powder Technol. **28**, 2126-2134 (2017).
DOI: https://doi.org/10.1016/j.apt.2017.05.019

[27] K. Rahmani, G.H. Majzoobi, The effect of particle size on microstructure, relative density and indentation load of Mg-B4C composites fabricated at different loading rates, J. Compos. Mater. **54**, 2297-2311 (2020).
DOI: https://doi.org/10.1177/0021998319896009

[28] C.A.V. Kumar, J.S. Rajadurai, Influence of rutile (TiO2) content on wear and microhardness characteristics of aluminium-based hybrid composites synthesized by powder metallurgy, Trans. Nonferrous Met. Soc. China (English Ed. **26**, 63-73 (2016).
DOI: https://doi.org/10.1016/S1003-6326(16)64089-X

[29] J. David Raja Selvam, D.S. Robinson Smart, I. Dinaharan, Microstructure and some mechanical properties of fly ash particulate reinforced AA6061 aluminum alloy composites prepared by compocasting, Mater. Des. **49**, 28-34 (2013).
DOI: https://doi.org/10.1016/j.matdes.2013.01.053

[30] Sudarshan, M.K. Surappa, Synthesis of fly ash particle reinforced A356 Al composites and their characterization, Mater. Sci. Eng. A. **480**, 117-124 (2008).
DOI: https://doi.org/10.1016/j.msea.2007.06.068

[31] V.S.S. Venkatesh, A.B. Deoghare, Fabrication and mechanical behaviour of Al-Kaoline metal matrix composite fabricated through powder metallurgy technique, Mater. Today Proc. **38**, 3291-3296 (2020). DOI: https://doi.org/10.1016/j.matpr.2020.10.021

[32] A. Baradeswaran, A. Elayaperumal, R. Franklin Issac, A statistical analysis of optimization of wear behaviour of Al- Al 2O3 composites using taguchi technique, Procedia Eng. **64**, 973-982 (2013). DOI: https://doi.org/10.1016/j.proeng.2013.09.174

[33] I. Balasubramanian, R. Maheswaran, Effect of inclusion of SiC particulates on the mechanical resistance behaviour of stir-cast AA6063/SiC composites, Mater. Des. **65**, 511-520 (2015).
DOI: https://doi.org/10.1016/j.matdes.2014.09.067